Mixed Convection of an Ag/Water Nanofluid in a Ventilated Square Cavity Containing Cold Blocks of Different Shapes

MERYEM BRAHIMI[1, 2], RAZIK BENDERRADJI[1, 3], HAMZA GOUIDMI[3]
[1]Department of Physics, Faculty of Sciences,
University of M'sila,
ALGERIA

[2]Laboratory of Materials and Renewable Energy (LMER),
University of M'sila,
ALGERIA

[3]Laboratory of Renewable Energy and Sustainable Development (LERDD),
University of Constantine 1,
ALGERIA

Abstract: - This research presents the results of a numerical study on mixed convection in a ventilated cavity with a central cold block of varying shapes. The direction of the forced flow of Ag/water nanofluid is perpendicular to the transverse axis (y) of the central cold block. Mixed convection is induced by cooling at the entrance of the ventilated cavity and uniformly heating its bottom wall. The governing equations for the flow of an incompressible Newtonian nanofluid are assumed to be two-dimensional, steady, and laminar. The finite volume method is employed for numerical simulations. A series of calculations are conducted to investigate the effects of key influencing factors: Reynolds number (Re = 100), Richardson number (Ri = 1), and nanoparticle volume fractions ($0 \leq \emptyset \leq 8\%$) on the enhancement of heat transfer. The impact of four different geometric shapes of the cold obstacle (circular, square, triangular, and elliptical) on fluid flow and heat transfer rate is also explored. The results indicate that an increase in nanoparticle volume fraction enhances the heat exchange rate in the cavity only when the geometric shape of the cold obstacle is circular. This is followed by square and triangular shapes, which approximately yield concordant results, and then the elliptical shape.

Key-Words: - Ventilated Square Cavity, Mixed Convection, Central cold Block, Nanofluid, Hybrid nanofluid Outlet port location, Heat transfer, Richardson number.

Received: April 29, 2023. Revised: November 18, 2023. Accepted: January 16, 2024. Published: April 1, 2024.

1 Introduction

In recent years, various methods have been employed to enhance mixed convection heat transfer in enclosures, sparking significant interest in numerous industrial applications such as process cooling, electronic components, radiators, heat exchangers, and more. One such method involves the use of nanofluids, which consist of colloidal suspensions of nanoscale solid particles (metallic or non-metallic) in a base fluid (such as water, oil, or ethylene glycol) to achieve improved thermal conductivity.

Several studies in this field have utilized different numerical methods. [1], aimed to review all published studies on mixed convection of nanofluids in enclosures. Papers were classified into four main categories: square (and rectangular) shapes, triangular shapes, trapezoidal shapes, and non-conventional shapes. Most studies reported a significant improvement in heat transfer with an increase in nanoparticle concentration, Reynolds number, and Richardson number, with the required pumping power increasing when adding nanoparticles to base fluids. Another numerical study was conducted by [2], presenting an investigation of mixed convection inside a trapezoidal cavity filled with Cu-water nanofluid under the influence of a constant magnetic field. Mixed convection is induced by the action of the inclined hot right-side wall in the direction of aiding or opposing flow. The left inclined side wall is fixed and maintained isothermal at a low temperature. The upper and lower horizontal walls are fixed and thermally insulated. The magnetic field is imposed

horizontally. Results showed that the suppressing effect of the magnetic field is more pronounced for the aiding case than for the opposing case. Meanwhile, the enhancement of the Nusselt number due to the presence of *Cu* nanoparticles is more significant for the opposing flow case. Heat transfer by mixed convection in an asymmetrically heated vertical channel filled with a mixture of water and two types of nanoparticles (*Cu, Al_2O_3*) was numerically investigated by [3]. Results indicated that the nanoparticle volume fraction with forced convection (induced by a heated channel wall) has a significant effect on nanofluid velocities and the average Nusselt number. *Cu-water* nanofluid exhibited better thermal performance than *Al_2O_3-water* nanofluid. Numerous studies have been conducted on mixed convection in a square cavity using nanofluids under various thermal and kinematic boundary conditions. As an example, [4], investigated stable conjugate mixed convection in a double-lid square cavity containing an internal solid body. The annulus is filled with Al_2O_3-water nanofluid based on the Buongiorno two-phase model. The upper horizontal wall is maintained at a constant low temperature and moves to the right, while the lower horizontal wall is maintained at a constant high temperature and moves to the left. The governing equations are numerically solved using the finite element method. Key parameters used in this study include internal solid body location, nanoparticle volume fraction ($0 \leq \varphi \leq 0.04$), Reynolds number ($1 \leq Re \leq 500$), Richardson number ($0.01 \leq Ri \leq 100$), solid body size ($0.1 \leq D \leq 0.7$), and solid body thermal conductivity (k_w = *0.01, 0.045, 0.1, 0.76, and 1.95 W/m℃*). Results showed a notable increase in heat transfer with the use of nanofluid in such a cavity. However, at low Reynolds numbers, adding nanoparticles had a negative effect on the Nusselt number when the Richardson number was very high. It was also observed that a large solid body could increase heat transfer in cases of high Reynolds and Richardson numbers. Additionally, several works have focused on the convective phenomenon of nanofluid in a ventilated square cavity. [5], numerically examined laminar steady mixed convection in a ventilated square cavity. The cavity is filled with different nanofluids and contains two ports for inflow and outflow. The right vertical wall is maintained at a hot temperature, while the other walls are considered adiabatic. Numerical simulations are performed for pure water fluid and mixtures of this basic fluid with nanoparticles (*Ag and Cu*) for Richardson numbers ranging from *0.04 to 4* and nanoparticle volume fractions between *0% and 10%*. This study is dedicated to a dynamic investigation with a fixed Grashof number of 10^4, varying Reynolds numbers. The numerical results obtained indicate an increase in heat transfer with an increase in the volume fraction, and the enhancement of the entropy generation and heat transfer product increases significantly with an increase in Reynolds number. The most effective nanoparticles for increasing the heat exchange rate are Ag, characterized by a high local Nusselt number, indicating excellent heat transfer compared to metallic *Cu* nanoparticles. In a similar context, [6], conducted a numerical simulation of convection in square-ventilated cavities containing insulated parallel baffles. The left and right walls of the cavity are maintained at a high temperature, while the upper and lower walls of the cavity, as well as the parallel baffles, are adiabatic. Opening slots are positioned in the upper and lower corners of the hot vertical walls. It was observed that the behavior of ventilated cavities depends not only on the size and position of the baffles but also strongly on the ventilation cavity configuration. Additionally, flow fields are limited by the larger baffle size, *Sb = 0.75*. However, few studies have addressed the case of a partially open cavity with an internal heat source, such as those by [7] , [8], which are related to the study of the effect of the Richardson number, the location of the exit orifice, and the nanoparticle volume fraction. The obtained results indicate that increasing the nanoparticle volume fraction and reducing the Richardson number improve the heat transfer rate. A study of forced, mixed, and natural convection of nanofluid inside a ventilated cavity with a central cold block of two different geometric shapes (square and triangular) was conducted by [9]. They numerically studied the effect of the Richardson number, different geometric shapes of the obstacle, and nanoparticle types. The results reveal that, in some cases, reducing the Richardson number and the size of solid particles improves heat transfer. It was also noted that there is an optimal concentration of nanoparticles at which the maximum average Nusselt numbers occur. This study is divided into two main aspects:

1. The effect of nanoparticle concentration.
2. The effect of the geometric shape of a central cold block.

Our results are presented in the form of isotherms and streamlines. They are displayed in temperature, velocity, local Nusselt number, and average Nusselt number profiles for different volume fractions.

2 Computational Model

2.1 Configuration

The studied configuration is depicted in Figure 1. It consists of a ventilated square-shaped cavity containing a cold block occupying the center of the cavity at a temperature (T_c). The block has different geometric shapes (circular, elliptical, square, and triangular) with the same peripheral surface area, diameter, and size, each equal to $D= 0.2H$. The cavity is uniformly heated; to a constant temperature (T_h) from the bottom wall, while the other walls are all thermally insulated (adiabatic walls). Our physical system is subjected to an external flow of nanofluid (Ag/water), introduced into the cavity with a velocity U_e and a temperature T_e ($T_e = (T_h + T_c)/2$), through an orifice placed at the upper level of the left wall, with dimensions ($h=0.1H$), and an outlet orifice of the same dimensions located at the bottom of the opposite wall.

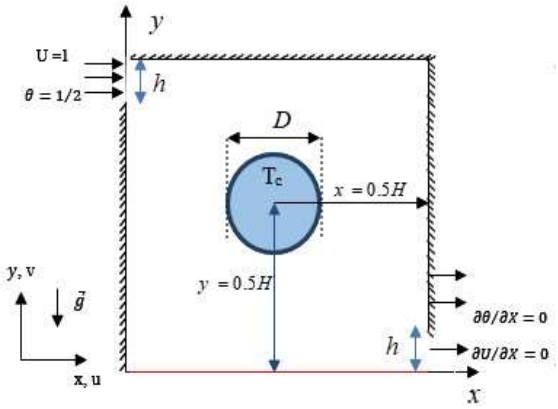

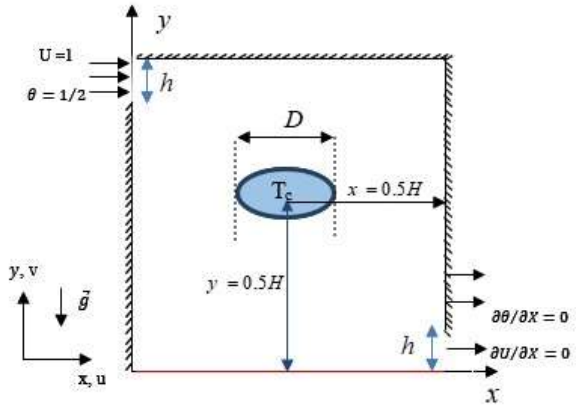

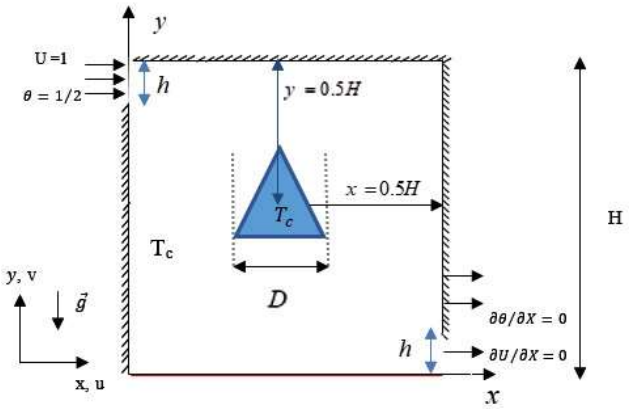

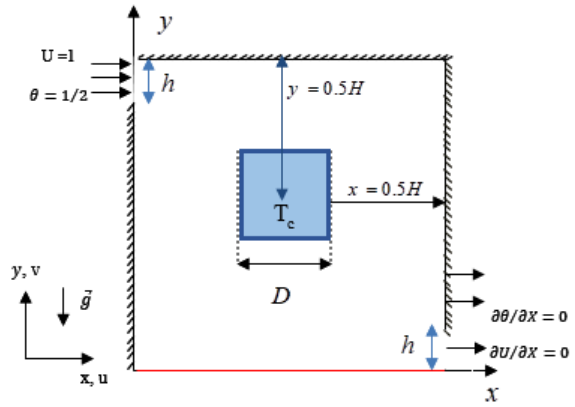

Fig. 1: The physical scheme of the problem and the boundary conditions

The flow is assumed Newtonian, incompressible in a steady laminar regime in a state of thermal equilibrium. According to the Boussinesq approximations, the density variation is neglected everywhere, except in the buoyancy term. The thermophysical properties with which we will work are shown in Table 1

.

Table 1. Thermophysical properties of water and nanoparticles with $T=300$ °K

	$\rho(Kg/m^3)$	$Cp\,(j/Kg.K)$	$k(/Kg.K)$	$\beta(K^{-1})$
H_2O	997.1	4179	0.613	21×10^{-5}
Ag	10500	235	429	1.89×10^{-5}

2.2 Governing Equations

According to the assumptions mentioned above, the equations governing the flow are the equation of continuity, momentum and energy, which can be written in the following dimensional form:

$$\frac{\partial U}{\partial x}+\frac{\partial V}{\partial y}=0 \quad (1)$$

$$u\frac{\partial u}{\partial x}+v\frac{\partial u}{\partial y}=\frac{1}{\rho_{nf}}\left(-\frac{\partial p}{\partial x}+\mu_{nf}\left(\frac{\partial^2 u}{\partial x^2}+\frac{\partial^2 u}{\partial y^2}\right)\right) \quad (2)$$

$$u\frac{\partial v}{\partial x}+v\frac{\partial v}{\partial y}=\frac{1}{\rho_{nf}}\left[-\frac{\partial p}{\partial y}+\mu_{nf}\left(\frac{\partial^2 v}{\partial x^2}+\frac{\partial^2 v}{\partial y^2}\right)+(\rho\beta)_{nf}g(T-T_c)\right] \quad (3)$$

$$u\frac{\partial T}{\partial x}+V\frac{\partial T}{\partial y}=\alpha_{nf}\left(\frac{\partial^2 T}{\partial x^2}+\frac{\partial^2 T}{\partial y^2}\right) \quad (4)$$

The properties of the nanofluid are calculated according to the following formulas, [10]:

The thermal diffusivity of nanofluid is:

$$\alpha_{nf}=\frac{k_{nf}}{(\rho C_p)_{nf}} \quad (5)$$

The density of a nanofluid is:

$$\rho_{nf}=(1-\varphi)\rho_f+\varphi\rho_s \quad (6)$$

The heat capacity of a nanofluid is:

$$(\rho C_p)_{nf}=(1-\varphi)(\rho C_p)_f+\varphi(\rho C_p)_s \quad (7)$$

The coefficient of thermal expansion of nanofluids can be determined by:

$$\beta_{nf}=(1-\varphi)\beta_f+\varphi\beta_s \quad (8)$$

According to Maxwell's model, the thermal conductivity of a nanofluid is:

$$\frac{k_{nf}}{k_f}=\frac{k_s+2k_f-2\varphi(k_f-k_s)}{k_s+2k_f+\varphi(k_f-k_s)} \quad (9)$$

The dynamic viscosity of a nanofluid is given by Brinkman (1952):

$$\mu_{nf}=\mu_f(1-\varphi)^{-2.5} \quad (10)$$

The boundary conditions of mixed convection are listed in the following Table 2:

Table 2. Hydrodynamic and thermal boundary conditions

Limit	Hydrodynamic conditions	Thermal conditions
Bottom wall	$u=0\,,v=0$	$T=T_h$
Upper wall	$u=0\,,v=0$	$\frac{\partial T}{\partial y}=0$
Straight wall	$u=0\,,v=0$	$\frac{\partial T}{\partial x}=0$
Left wall	$u=0\,,v=0$	$\frac{\partial T}{\partial x}=0$
Hall	$u=U_e\,,v=0$	$T=\frac{T_h+T_c}{2}$
Exit	$\frac{\partial u}{\partial x}=0\,,v=0$	$\frac{\partial T}{\partial x}=0$
block	$u=0\,,v=0$	$T=T_c$

The reduced variables used during dimensioning of equations (1-4) as well as the Reynolds, Grashof, Prandtl and Richardson numbers are respectively given by the following expressions:

$$X=\frac{x}{H}\,,\ Y=\frac{y}{H}\,,\ U=\frac{u}{U_0}\,,\ V=\frac{v}{U_0}\,,\ P\frac{p}{\rho V_0^2}\,,\ \theta=\frac{T-T_c}{T_h-T_c} \quad (11)$$

$$Re=\frac{UH}{v_f}\,,\quad Gr=\frac{g\beta_f(T_h-T_c)H^3}{v_f^2}\,,\quad Pr=\frac{v_f}{\alpha_f}\,,\quad Ri=\frac{Gr}{Re^2} \quad (12)$$

By carrying the dimensionless quantities defined above in the equations of the mathematical model (1), (2), (3) and (4), we obtain:

$$\frac{\partial U}{\partial X}+\frac{\partial V}{\partial Y}=0 \quad (13)$$

$$U\frac{\partial U}{\partial X}+V\frac{\partial U}{\partial Y}=-\frac{\partial P}{\partial X}+\frac{1}{Re}\frac{\rho_f}{\rho_{nf}}\frac{\mu_{nf}}{\mu_f}\left[\frac{\partial^2 U}{\partial X^2}+\frac{\partial^2 U}{\partial Y^2}\right] \quad (14)$$

$$U\frac{\partial V}{\partial X}+V\frac{\partial V}{\partial Y}=-\frac{\partial P}{\partial Y}+\frac{1}{Re}\frac{\rho_f}{\rho_{nf}}\frac{\mu_{nf}}{\rho_{nf}}\left[\frac{\partial^2 V}{\partial X^2}+\frac{\partial^2 V}{\partial Y^2}\right]+Ri\frac{(\rho\beta)_{nf}}{\rho_{nf}\beta_f}\theta \quad (15)$$

$$U\frac{\partial\theta}{\partial X}+V\frac{\partial\theta}{\partial Y}=\frac{1}{Re.Pr}.\frac{\alpha_{nf}}{\alpha_f}.\left(\frac{\partial^2\theta}{\partial X^2}+\frac{\partial^2\theta}{\partial Y^2}\right) \quad (16)$$

The dimensionless boundary conditions relating to our physical domain are shown in the following Table 3:

Table 3. Dimensionless hydrodynamic and thermal boundary conditions

Limit	Hydrodynamic conditions	Thermal conditions
Bottom wall	$U=0, V=0$	$\theta=1$
Upper wall	$U=0, V=0$	$\frac{\partial\theta}{\partial Y}=0$
Straight wall	$U=0, V=0$	$\frac{\partial\theta}{\partial X}=0$
Left wall	$U=0, V=0$	$\frac{\partial\theta}{\partial X}=0$
Hall	$U=1, V=0$	$\theta=1/2$
Exit	$\frac{\partial U}{\partial X}=0, V=0$	$\frac{\partial\theta}{\partial X}=0$
block	$U=0, V=0$	$\theta=0$

The local Nusselt number (Nu) along the lower hot wall can be expressed by:

$$Nu=-\frac{k_{nf}}{k_f}.\frac{\partial\theta/\partial n}{T_h-T_c}.H \quad (18)$$

The average value of the Nusselt number along this wall is calculated by the following integral:

$$\overline{Nu}=\frac{1}{H}\int_0^H\frac{k_{nf}}{k_f}\left\{\left|\frac{\partial\theta}{\partial Y}\right|_{Y=0}\right\}dX \quad (19)$$

3 Numerical Method

To solve the equations governing this problem, we employed the SIMPLE algorithm along with the second-order scheme of the finite volume method. The computations were carried out using the Ansys-Fluent 6.3 software.

3.1 Mesh Independence

A quadratic cell mesh is utilized for this study. The mesh is meticulously designed to refine near the block and adjacent walls, gradually coarsening as it extends farther away from both. This strategy aims to reduce the overall computational cost while enhancing the precision of the simulation results. As established in the Table 4, four different meshes are selected—100 x 160, 110 x 180, 120 x 200, and 130 x 200 nodes—to analyze the effect of the number of nodes, enabling the attainment of highly accurate solutions without compromising computational time.

Table 4. Flow characteristics for different grids ((*Cu/water*), φ*=0.05, Re=100, Ri= 0.1*)

Mesh	100 × 160	110 × 180	120 × 200	130 × 220
$\mathbf{Nu}_{avg}$	21.600	21.676	21.717	21.701

3.2 Code Validation

To validate the code governing this simulation, a comparison was made between the average Nusselt values obtained in this work and those calculated by [11]. This corresponds to cases of a rectangular cavity with a central square-shaped obstacle, maintained at a hot temperature (Th = 310 °K). The cavity was filled with a water-based nanofluid containing Cu nanoparticles. The left and right vertical walls of the cavity were cooled to constant temperatures (Tc = 290 °K), while the upper and lower walls were considered adiabatic.

The comparison is conducted for a specific case with a Rayleigh number (Ra) of (10^4 and 10^6) and a nanoparticle volume fraction (φ) of 5%. Some values of this comparison are gathered in Figure 2. The results are highly compatible as they converge well, and the margin of error is extremely minor. This validation enhances confidence in the accuracy of our numerical simulations and strengthens the credibility of the results obtained in this study.

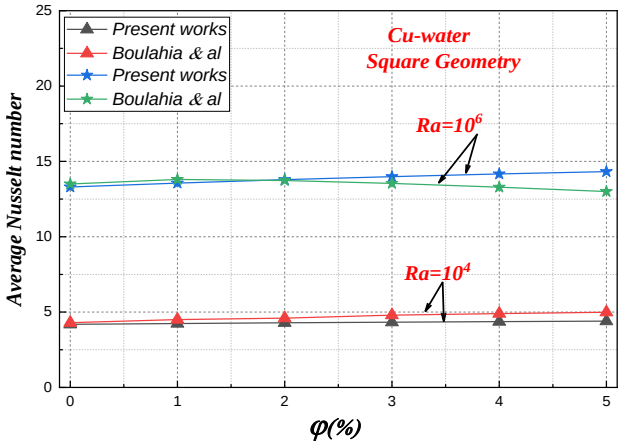

Fig. 2: Evolution of the average Nusselt number along the hot wall. Comparison of the present numerical study with the data processed by [11]

4 Results and Discussion

In this section, the numerical results are presented in terms of stream function and isotherm contours, average Nusselt number, temperature profiles, and velocity profiles for a range of volume fraction values (φ = 0, 2, 4, 6, 8%), Reynolds number Re = 100, and Richardson number Ri = 1. The streamlines and isotherms for some cases studied in this work (φ= 4%, Re=100, Ri= 1.) are presented in Figure 3. In general, it can be observed that the nanofluid flow maintains the same structure for all geometric shapes of the central obstacle, where the flow is directed from the inlet port upward and downward of the obstacle, then moves toward the outlet port. The incoming flow strikes the left side of the central obstacle and distributes it to almost the same geometric shape, producing recirculation zones that rotate clockwise. The recirculation zones form near the inlet port, and these vortices increase in size when the obstacle is circular (Case B) compared to other obstacles (Square (Case A), Triangle (Case C), Ellipse (Case D)).

This can be explained by the higher resistance of the square and triangular blocks to fluid circulation within the ventilated cavity, indicating that the circular geometric shape has a remarkable effect on enhancing mixed convection by improving heat transfer. For the isotherms, the color representation varies from blue to red. The blue color represents low-temperature zones, while red corresponds to high temperatures. The temperature field is presented at the bottom of Figure 3, which shows that high temperatures are localized in narrow spaces near the hot wall, corresponding to the thickness of the thermal boundary layer (Red part in the mentioned figure). This indicates good heat exchange through convection (mixed convection). There is also an increase in the cold zone, and the isotherms are less tightly packed on the hot wall in case B (circle obstacle), compared to the other cases (A, C, D), due to the effect of the geometric shape exchange of the cold obstacle

It is also noted that the cold obstacle at the center of the cavity acts as a cold source and leads to the concentration of high-temperature regions near its walls. As long as the flow is directed from the inlet port upwards to the outlet port downwards, and during this path, it strikes the left side of the central obstacle, the isotherms move downward. Comparing the streamlines in the figure, it can be seen that the obstacle causes the appearance of vortices. This dynamic phenomenon results in the manifestation of wavelike isotherms inside the cavity. The magnitude of the heat transfer rate, deduced from the isotherms, is influenced by both the geometry of the cold obstacle and the inlet velocity of the nanofluid. Furthermore, the position of these heat transfer fluctuations depends on the inlet port's position (top, bottom, or in the middle). Moreover, the ventilation of the nanofluid inside the cavity leads to the extension of the isotherms toward the outlet port. This observation aligns with the results obtained from the analysis of the Nusselt number.

Figure 4 shows the effect of increasing the volume fraction of nanoparticles in the nanofluid ($\boldsymbol{\varphi}$) on the average Nusselt number for four geometric shapes of the obstacle. It is evident that increasing the nanoparticle concentration enhances the heat transfer rate, leading to a rising trend in the average Nusselt number. This is attributed to the improvement in the effective thermal conductivity of the nanofluid with the addition of nanoparticles. The agitation of particles near the obstacle promotes heat transfer between the cold obstacle and the nanofluid. Furthermore, it can be observed that the values of the average Nusselt number for the circular-shaped obstacle are higher than those for other shapes. This is indeed due to the effect of the resistance of nanofluid circulation within the ventilated cavity, resulting from the geometric shape

exchange of the central cold obstacle. The lowest Nusselt value is, as expected, recorded when the obstacle has an elliptical geometric shape.

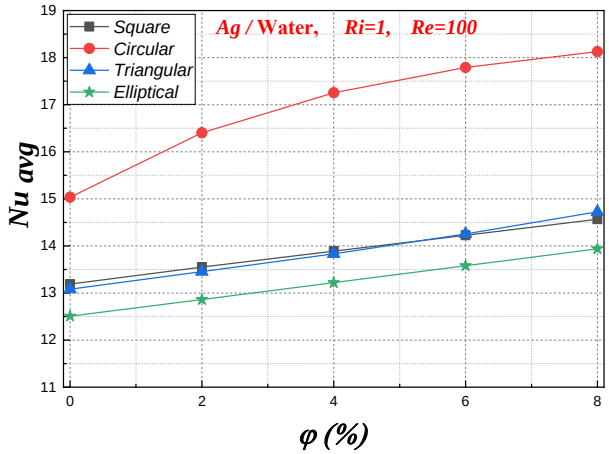

Fig. 4: Variation of the average Nusselt number for different volume fractions (φ %) and different geometric shapes of the cold obstacle for (Ag/Water)

impact of nanoparticle volume fractions on heat transfer enhancement was examined.

Four different geometric shapes for the cold obstacle (circle, square, triangle, and ellipse) were considered. The results showed that:

1. Increasing nanoparticle volume fractions had a positive impact on heat transfer, leading to an increase in the average Nusselt number. Circular obstacles consistently exhibited higher Nusselt numbers compared to other shapes, highlighting the influence of geometric shapes on nanofluid circulation and heat transfer.
2. The central cold obstacle acted as a cold source, concentrating high-temperature regions near its walls. The dynamic flow around the obstacle caused the appearance of vortices, resulting in wavelike isotherms inside the cavity.
3. Isotherms, representing temperature variations, showed that circular obstacles facilitated better heat exchange, with less tightly packed isotherms on the hot wall compared to other shapes. The circular shape contributed to enhanced mixed convection and strengthened heat transfer.

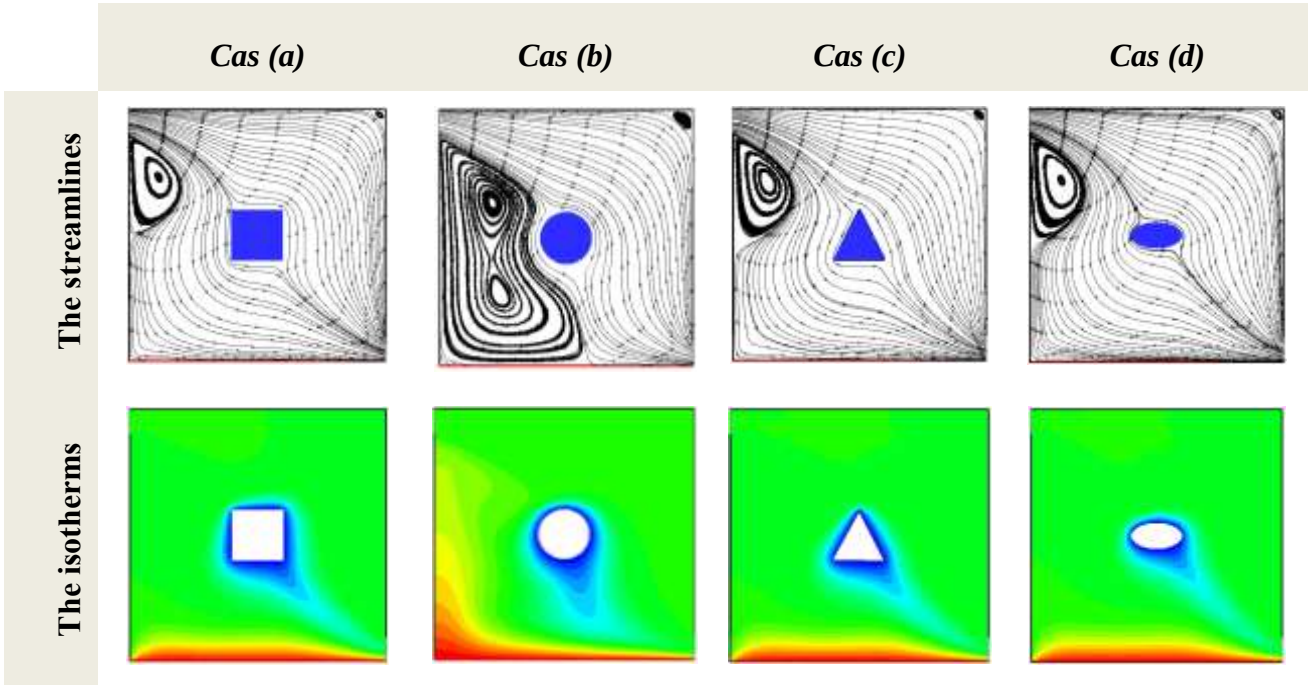

Fig. 3: Streamlines and isotherms for different geometric shapes of the cold obstacle (Ag/Water), for φ=4%, Re=100, Ri=1

5 Conclusion

The heat transfer rate and flow structures of an Ag/H2O nanofluid cooling a ventilated square cavity containing a central cold block of various shapes were numerically investigated, and the

The study provides insights into the role of geometric shape and nanoparticle concentration in improving heat transfer by mixed convection. Practical applications could benefit from optimizing

the design of cold obstacles and controlling nanoparticle concentrations to achieve enhanced heat exchange rates, offering valuable information for applications in various industrial contexts, such as cooling electronic components and industrial processes.

References:

[1] Izadi, S., Armaghani, T., Ghasemiasl, R., Chamkha, A. J. and Molana, M.. A comprehensive review on mixed convection of nanofluids in various shapes of enclosures. *Powder Technology*, 343, 880-907. (2018), https://doi.org/10.1016/j.powtec.2018.11.006

[2] Chamkha, A. J., & Ismael, M. A. Magnetic Field Effect on Mixed Convection in Lid-Driven Trapezoidal Cavities Filled With a Cu–Water Nanofluid With an Aiding or Opposing Side Wall. *Journal of Thermal Science and Engineering Applications*, *8*(3). (2016), https://doi.org/10.1115/1.4033211

[3] Bouhezza, A., Kholai, O. and Teggar, M.. Numerical investigation of nanofluids mixed convection in a vertical channel. *Mathematical Modelling of Engineering Problems*, 6(4), 575-580. (2019), https://doi.org/10.18280/mmep.060413.

[4] Alsabery, A. I., Ismael, M. A., Chamkha, A. J. and Hashim, I.. Mixed convection of Al 2 O 3 -water nanofluid in a double lid-driven square cavity with a solid inner insert using Buongiorno's two-phase model. *International Journal of Heat and Mass Transfer*, 119, 939-961. (2018) DOI:10.1016/J.IJHEATMASSTRANSFER.2017.11.136

[5] Benderradji, R., Brahimi, M. and Khalfallah, F.. Numerical Study of Heat Transfer by Mixed Convection in a Cavity Filled With Nanofluid: Influence of Reynolds and Grashof Numbers. *International Journal of Applied Mathematics Computational Science and Systems Engineering*, 4, 77-86. (2022), http://dx.doi.org/10.37394/232026.2022.4.10

[6] Palaniappan, G., Murugan, M., Al-Mdallal, Q.M., Abdalla, B. and Doh, D.H.. Numerical investigation of open cavities with parallel insulated baffles. *International Journal of Heat and Technology*, 38(3), 611-621. (2020), https://doi.org/10.18280/ijht.380305.

[7] Mehrizi, A. A., Farhadi, M., Afroozi, H. H., Sedighi, K. and Darz, A. A. R.. Mixed convection heat transfer in a ventilated cavity with hot obstacle: Effect of nanofluid and outlet port location. *International Communications in Heat and Mass Transfer*, 39(7), 1000-1008. (2012), 10.1016/j.icheatmasstransfer.2012.04.002.

[8] Boulahia, Z., Wakif, A. and Sehaqui, R.. Heat transfer and cu-water nanofluid flow in a ventilated cavity having a central cooling cylinder and heated from the below considering three different outlet port locations. *Frontiers in Heat and Mass Transfer*, 11, 11. (2018), http://dx.doi.org/10.5098/hmt.11.11.

[9] Boulahia, Z., Wakif, A., Chamkha, A. J. and Sehaqui, R.. Numerical study of forced, mixed and natural convection of nanofluids inside a ventilated cavity containing different shapes of cold block. *Journal of Nanofluids*, 8(2), 439-447. (2019), http://dx.doi.org/10.1166/jon.2019.1598.

[10] Oztop, H. F. and Abu-Nada, E.. Numerical study of natural convection in partially heated rectangular enclosures filled with nanofluids. *International Journal of Heat and Fluid Flow*, 29(5), 1326–1336. (2008), https://doi.org/10.1016/j.ijheatfluidflow.2008.04.009.

[11] Boulahia, Z., Wakif, A. and Sehaqui, R.. Finite volume analysis of free convection heat transfer in a square enclosure filled by a Cu-water nanofluid containing different shapes of heating cylinder. *Journal of Nanofluids*, 6(4), 761-768. (2017), https://doi.org/10.1166/jon.2017.1363.

Contribution of individual authors to the creation of a scientific article (ghostwriting policy)

All authors equally contributed in the present research.

Sources of Funding for Research Presented in a Scientific Article or Scientific Article Itself

No funding was received for conducting this study.

Conflict of Interest

The authors have no conflicts of interest to declare.